Lecture NO (11)
Fluid Friction in Pipes

11.1. Introduction

In chemical engineering process operations, fluids are typically conveyed through pipelines, in which viscous action—with or without accompanying turbulence—leads to “friction” and a dissipation of useful work into heat. Such friction is normally overcome either by means of the pressure generated by a pump or by the fluid falling under gravity from a higher to a lower elevation. In both instances, it is usually necessary to know what flow rate and velocity can be expected for a given driving force.Fig. 11.1 shows a pipe fitted with pressure gauges that record the pressures p_1 and p_2 at the beginning and end of a test section of length L. A horizontal pipe is intentionally chosen because the observations are not then complicated by the effect of gravity. In addition, for good results, it is desirable that a substantial length of straight pipe should precede the first pressure gauge, in order that the flow pattern is fully developed (no longer varying with distance along the pipe) at that location.

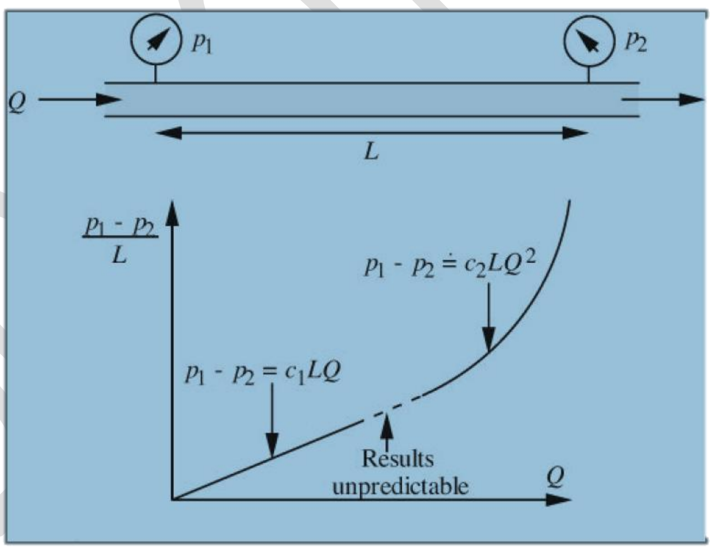

Fig. 11.1 Pressure drop in a horizontal pipe.

For a given flow rate, repetition of the experiment for different lengths demonstrates that the pressure drop $(p_1 - p_2)$ is directly proportional to L. Hence, it is appropriate to plot the pressure drop per unit length $(p_1 - p_2)/L$ (the negative of the *pressure gradient dp/dz*, where z denotes distance along the pipe) against the volumetric flow rate Q. There are three distinct flow regimes in the resulting graph:

1. For flow rates that are low (in a sense to be defined shortly), the pressure gradient is directly proportional to the flow rate.

2. For intermediate flow rates, the results are irreproducible, and alternate seemingly randomly between extensions of regimes 1 and 3.

3. For high flow rates, the pressure gradient is closely proportional to the *square* of the flow rate. These regimes are known as the *laminar*, *transition*, and *turbulent* zones, respectively. The situation is further illuminated by the famous 1883 experiment of Sir Osborne Reynolds (see box above), similar to that illustrated in Fig. 11.2, where a liquid flow in a transparent tube.

1. For low flow rates, Fig. 11.2(a), the injected dye jet maintains its integrity as a long filament that travels along with the liquid. (The jet actually broadens gradually, due to diffusion.)

2. For intermediate flow rates, the results are irreproducible, and seem to alternate between extensions of regimes 1 and 3.

3. For high flow rates, Fig. 11.2(b), the jet of dye mixes very rapidly with the surrounding liquid and becomes highly diluted, so that it soon becomes invisible. The reason is that the liquid flow in the pipe is *unstable*, consisting of random turbulent motions superimposed on the bulk flow to the right.

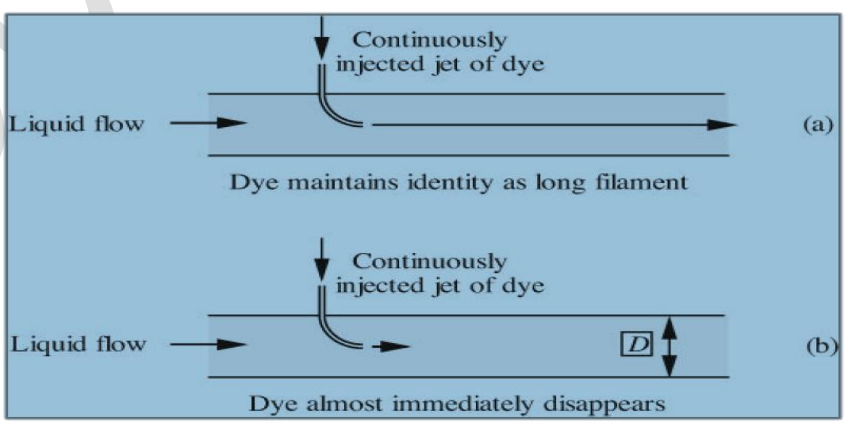

Fig. 11.2 The Reynolds experiment.

Further experiments show that the three regimes do not depend solely on the flow rate, but on a dimensionless *combination* of the mean fluid velocity um, its density ρ and viscosity μ, and the diameter *D* of the pipe. The combination or *dimensionless group* is defined by:

$$Re = \frac{\rho u D}{\mu} \dots\dots\dots\dots\dots\dots\dots\dots\dots\dots (11.1)$$

and is called the Reynolds number, and indicates the relative importance of inertial effects. Table 3.1 shows which regime can be expected for a given Reynolds number. The exponent on Q is 1.8 or 2, depending on whether the pipe is hydraulically smooth or rough, respectively, in a sense to be defined later. In Sections 11.2 and 11.3 we shall study flow in the laminar and turbulent regimes more closely.

Table 11.1 Dependence of Pipe Flow Regime on the Reynolds Number

Approximate Value of Reynolds Number	Flow Regime	Pressure Gradient is Proportional to
< 2000	Laminar	Q
2000 – 4000	Transition	Variable
> 4000	Turbulent	$Q^{1.8} - Q^{2}$

11.2. Laminar Flow

In order to avoid the additional complication of gravity (which will be included later), consider flow in the horizontal cylindrical pipe of radius a shown in Fig. 11.3.

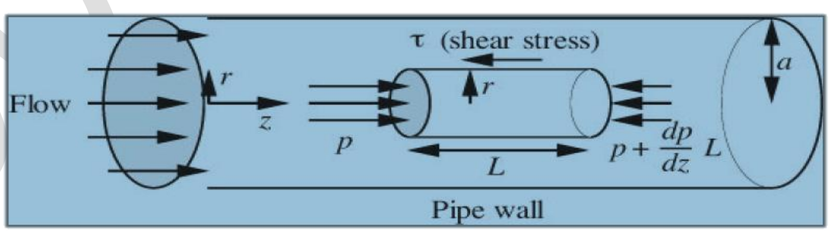

Fig. 11.3 Forces acting on a cylindrical fluid element.

Consider further a moving cylinder of fluid of radius *r* and length *L*. In this case, there is zero *convective* transport of momentum across the two circular ends of the cylinder, and the analysis is simplified. The net pressure force acting on the circular area $\boldsymbol{\pi r^2}$ of the two ends is exactly counterbalanced by the shear stress acting on the curved surface, of area $\boldsymbol{2\pi r L}$.

Thus, a steady-state momentum balance to the right gives:

$$p\pi r^2 - \left(p - \frac{p}{dz}L\right)\pi r^2 - \tau 2\pi r L = 0 \dots\dots\dots\dots\dots (11.2)$$

Simplifying,

$$\tau = \frac{r}{2}\left(-\frac{dp}{dz}\right) \dots\dots\dots\dots\dots\dots\dots\dots\dots\dots\dots (11.3)$$

Eqn. (11.3) may be used for finding the shear stress at any radial location

The analysis so far holds equally well for laminar or turbulent flow. However, specializing now to the case of laminar flow of a Newtonian fluid, the shear stress is directly proportional to the velocity gradient:

$$\tau = -\mu \frac{du}{dr} \dots\dots\dots\dots\dots\dots\dots\dots\dots\dots (11.4)$$

Elimination of τ between Eqns. (11.3) and (11.4) gives:

$$-\mu \frac{du}{dr} = \frac{r}{2}\left(-\frac{dp}{dz}\right) \dots\dots\dots\dots\dots\dots\dots\dots\dots\dots (11.5)$$

which integrates to:

$$\int_0^u du = -\frac{1}{2\mu}\left(-\frac{dp}{dz}\right)\int_a^r r\,dr \dots\dots\dots\dots\dots.. (11.6)$$

in which the boundary condition of u = 0 at r = a reflects a condition of no slip at the pipe wall. The final expression for the velocity u at any radial location r is:

$$u = \frac{1}{4\mu}\left(-\frac{dp}{dz}\right)(a^2 - r^2) \dots\dots\dots\dots\dots.. (11.7)$$

Observe that the pressure gradient can be expressed in terms of the total pressure drop $-\Delta p$ over a finite length L, as follows:

$$\frac{dp}{dz} = \frac{p_2 - p_1}{L} = -\frac{p_1 - p_2}{L} = \frac{\Delta p}{L} \dots\dots.. (11.8)$$

Hence, the velocity profile can also be rewritten as:

$$u = \frac{-\Delta p}{4\mu L}(a^2 - r^2) \dots\dots\dots\dots\dots\dots\dots\dots.. (11.9)$$

The total volumetric flow rate Q is obtained by integration over the cross section of the pipe. Consider the differential annulus of internal radius r and width dr shown in Fig. 3.4. Its area may be obtained in either of two ways:

(a) as the difference in areas between two circles of radii **r + dr** and **r**, neglecting a term in **(dr)**^{2}; or (b) by "unwinding" the annulus and regarding it as a rectangular strip of length 2πr and width dr. The area ***dA*** and the corresponding flow rate ***dQ*** through it are:

$$dA = \pi(r+dr)^2 - \pi r^2 = \pi r^2 + 2\pi r dr + \pi(dr)^2 - \pi r^2 = 2\pi r dr \text{ ……….} (11.10a)$$

$$dA = 2\pi r dr \text{ ………………………………………………………} (11.10b)$$

$$dQ = udA = 2\pi r u dr \text{ ……………………………………………} (11.11)$$

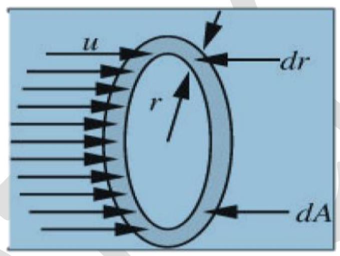

Fig. 11.4 Flow through a differential

$$Q = \int_0^Q dQ = 2\pi \int_0^a \underbrace{\frac{1}{4\mu}\left(-\frac{dp}{dz}\right)}_{Constant} (a^2 - r^2) r dr$$

$$= \frac{\pi a^4}{8\mu}\left(-\frac{dp}{dz}\right) = \frac{\pi a^4}{8\mu}\frac{p_1 - p_2}{L} \text{ ………………………….} (11.12)$$

relation for pipe flow known as the ***Hagen-Poiseuille law.***

The above analysis can also be extended to the case of an *inclined* pipe, again by performing a momentum balance, but now including a gravitational force. The pressure gradient would be supplemented by the term $\pm \rho g \sin\theta$, and the result for the velocity profile, for example, would be:

$$u = \frac{1}{4\mu}\left(-\frac{dp}{dz} \pm \rho g sin\theta\right) = (a^2 - r^2) \text{ ………………………….} (11.13)$$

where θ is the (positive) angle of inclination to the horizontal. The plus sign in Eqn. (11.13) holds for downhill flow, and the minus sign for uphill flow. The velocity profile will still be parabolic, regardless of the orientation of the pipe.

Frictional dissipation term *F*. An alternative and generally more useful approach is first to establish the *frictional dissipation* term for a horizontal pipe, shown in Fig. 11.5.

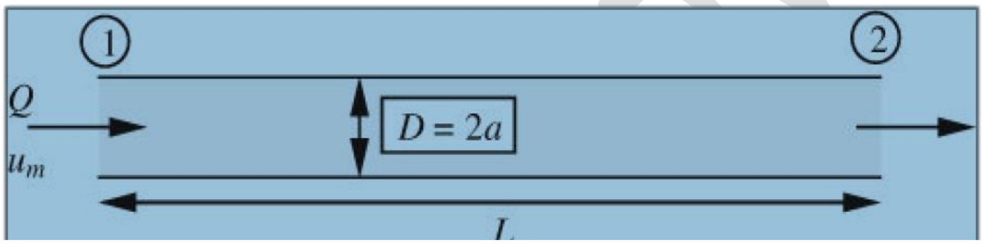

Fig. 11.5 Flow in a horizontal pipe.

The Hagen-Poiseuille law can be rephrased as:

$$Q = \frac{\pi a^4(-\Delta p)}{8\mu L} \ldots\ldots\ldots\ldots\ldots\ldots\ldots\ldots\ldots\ldots (11.14)$$

where $\Delta p = p_2 - p_1$ (as always, "Δ" denotes the final minus the initial value). But an overall energy balance.

$$\alpha\Delta\left(\frac{u^2}{2}\right) + g\Delta z + \frac{\Delta p}{\rho} + w + f = 0 \ldots\ldots (11.15)$$

in which the factor α is unimportant at present but will be explained shortly. The first, second, and fourth terms are zero because there is no change in velocity, no change in elevation, and no work performed. Solution for f and elimination of Δp using Eqn. (11.14) gives:

$$f = \frac{\Delta p}{\rho} = \frac{8\mu LQ}{\pi a^4 \rho} = \frac{8\mu u_m L}{a^2 \rho} \ldots\ldots\ldots\ldots\ldots\ldots\ldots\ldots\ldots\ldots (11.16)$$

This expression for F is "universal" in the sense that it does not depend on the inclination of the pipe; it may therefore be used in the energy balance for flow in horizontal, inclined, or vertical pipes. The reason is that the frictional dissipation depends on the magnitude and shape of the velocity profile, which is parabolic in all instances, and does not depend on the pipe orientation. The following relations are also available:

Maximum velocity

The fluid velocity is greatest at the centerline, and substitution of r = 0 into Eqn. (11.7) gives:

$$u_{max} = \frac{a^4}{4\mu}\left(-\frac{dp}{dz}\right) \dots\dots\dots\dots\dots\dots..(11.17)$$

Mean velocity

The mean velocity of the fluid is obtained by dividing the total flow rate from Eqn. (11.12) by the cross-sectional area, and equals half the maximum velocity:

$$u_m = \frac{Q}{\pi a^2} = \frac{\pi a^2}{8\mu}\left(-\frac{dp}{dz}\right) = \frac{1}{2}u_{max} \dots.(11.18)$$

Kinetic energy per unit mass

For purposes of overall energy balances, we need to find the kinetic energy associated with a unit mass of fluid as it traverses a particular axial location z. It will be seen that this is not simply half the square of the mean velocity, $\frac{u_m^2}{2}$.

For any general property ψ per unit mass ($\psi = u^2/2$ in the case of kinetic energy), define an average value $\bar{\psi}$ per unit mass flowing as:

$$\bar{\psi} = \frac{\underbrace{\int_0^a \underbrace{2\pi r dr}_{dA}\ (\rho u \psi)}_{Total\ amount\ of\ \psi\ flowing}}{\underbrace{\int_0^a \underbrace{2\pi r dr}_{dA}\ (\rho u)}_{Total\ mass\ flow\ rate}} \dots\dots\dots\dots\dots\dots\dots.(11.9)$$

Substitution of $\psi = u^2/2$ into Eqn. (11.19) and recognizing that the denominator is simply ρQ gives the kinetic energy per unit mass flowing:

Thus, the

$$\overline{KE} = \frac{1}{\rho Q}\int_0^a 2\pi r dr\ \left(\rho u \frac{u^2}{2}\right) = \left[\frac{a^2}{8\mu}\left(-\frac{dp}{dz}\right)\right]^2 = u_m^2 \left(not\ \frac{u_m^2}{2}\right) \dots\dots\dots.(11.20)$$

Thus, the kinetic energy per unit mass in laminar pipe flow is:

$$\overline{KE} = \alpha \frac{u_m^2}{2} \dots\dots\dots\dots\dots\dots\dots\dots\dots\dots\dots\dots\dots\dots\dots\dots\dots (11.21)$$

in which α = 2.

For *turbulent* velocity profiles, the integration of (11.19) is still performed with $\psi = u^2/2$, but now with a velocity profile that is appropriate for turbulent flow. Compared to their laminar counterparts, turbulent velocity profiles are much flatter near the centerline and steeper near the wall, and the result is $\alpha \doteq 1.07$. Further, since the kinetic energy term is frequently small when compared with other terms in the energy balance, α can usually safely be taken as unity for turbulent flow, and will therefore often be omitted.

By focusing on the shear stress τ_w at the wall, Eqn. (11.22) can be rephrased by asserting that in turbulent flow, the dimensionless wall shear stress or friction factor:

$$f = \frac{\tau_w}{\rho u_m^2} \dots\dots\dots\dots\dots\dots\dots\dots\dots\dots\dots (11.22)$$

Other versions in more common use are the Fanning friction factor:

$$f_F = \frac{\tau_w}{\frac{1}{2}\rho u_m^2} \dots\dots\dots\dots\dots\dots\dots\dots\dots\dots (11.23)$$

and the Moody friction factor:

$$f_M = \frac{\tau_w}{\frac{1}{8}\rho u_m^2} \dots\dots\dots\dots\dots\dots\dots\dots\dots\dots\dots (11.24)$$

11.3. Piping and Pumping Problems

Upward flow in an inclined pipe is depicted in Fig. 11.6. A steady-state momentum balance in the direction of flow on the fluid in the pipe gives:

$$\underbrace{p_1 - p_2 \frac{\pi D^2}{4}}_{Net\ pressure\ force} - \underbrace{\tau_w \pi D L}_{Wall\ shearstress\ force} - \underbrace{\frac{\pi D^2}{4} \rho L g sin\theta}_{Gravitational force} = 0 \dots\dots\dots (11.25)$$

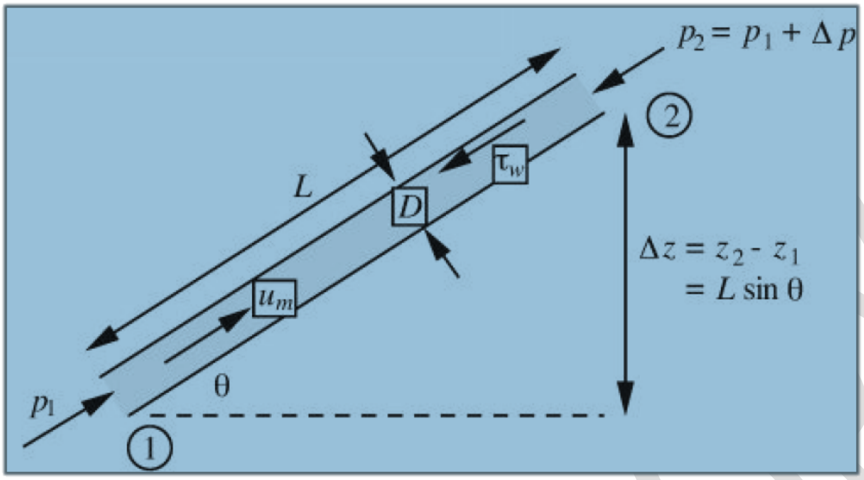

Fig. 11.6 Pressure drop in an inclined pipe.

Here, the three terms are the net pressure force that drives the flow, the retarding shear force exerted by the pipe wall, and the retarding gravitational weight of the fluid. Equation (11.25) can be rewritten as:

$$-\Delta p = p_1 - p_2 = 4\tau_w \frac{L}{D} + \rho g \Delta z \dots\dots\dots\dots\dots\dots\dots\dots\dots\dots (11.26)$$

But, from the definition of the Fanning friction factor, Eqn.(11.23)

$$\tau_w = \frac{1}{2} f_F \rho u_m^2 \dots\dots\dots\dots\dots\dots\dots\dots\dots\dots\dots\dots\dots (11.27)$$

Elimination of the wall shear stress between Eqns. (11.26) and (11.27) gives:

$$-\Delta p = p_1 - p_2 = \underbrace{2 f_F \rho u_m^2 \frac{L}{D}}_{Friction} + \underbrace{\rho g \Delta z}_{Gravity} = \frac{32 f_F \rho Q L}{\pi^2 D^5} + \rho g \Delta z \dots\dots (11.28)$$

An alternative and somewhat more generally useful form of Eqn. (3.33) is obtained by investigating the frictional dissipation per unit mass. Rearrangement of Eqn. (11.28) gives:

$$g\Delta z + \frac{\Delta p}{\rho} + 2 f_F \rho u_m^2 \frac{L}{D} = 0 \dots\dots\dots\dots\dots\dots\dots\dots\dots\dots\dots (11.29)$$

But the overall (incompressible) energy balance

$$\underbrace{\Delta\left(\frac{u^2}{2}\right)}_{zero} + g\Delta z + \frac{\Delta p}{\rho} + \underbrace{w}_{zero} + f = 0 \ldots\ldots\ldots\ldots\ldots\ldots\ldots. (11.30)$$

Note that there is zero change in kinetic energy for pipe flow because the velocity is constant, and also that there is no work in the absence of a pump or turbine. A comparison of Eqns. (11.29) and (11.30) immediately gives the frictional dissipation per unit mass:

$$f = 2f_F u_m^2 \frac{L}{D} = \frac{32 f_F Q^2 L}{\pi^2 D^5} \ldots\ldots\ldots\ldots\ldots\ldots\ldots\ldots\ldots\ldots\ldots\ldots\ldots\ldots\ldots\ldots\ldots (11.31)$$

a result that is valid for laminar or turbulent flow.

However, for the special case of laminar flow, we know from Eqn. (11.16) that:

$$f = 2f_F u_m^2 \frac{L}{D} = \frac{8\mu u_m L}{a^2 \rho} \ldots\ldots\ldots\ldots\ldots\ldots\ldots\ldots\ldots\ldots (11.32)$$

Since a = D/2, the friction factor for laminar flow is therefore:

$$f_F = \frac{16\mu L}{u_m \rho D} = \frac{16}{Re} \ldots.\ldots\ldots\ldots\ldots\ldots (11.33)$$

Experimentally, the friction factor f_F depends on the Reynolds number Re and—if the flow is turbulent—on the pipe roughness ratio ε /D. The salient features are shown in the friction-factor plot of Fig. 11.7.

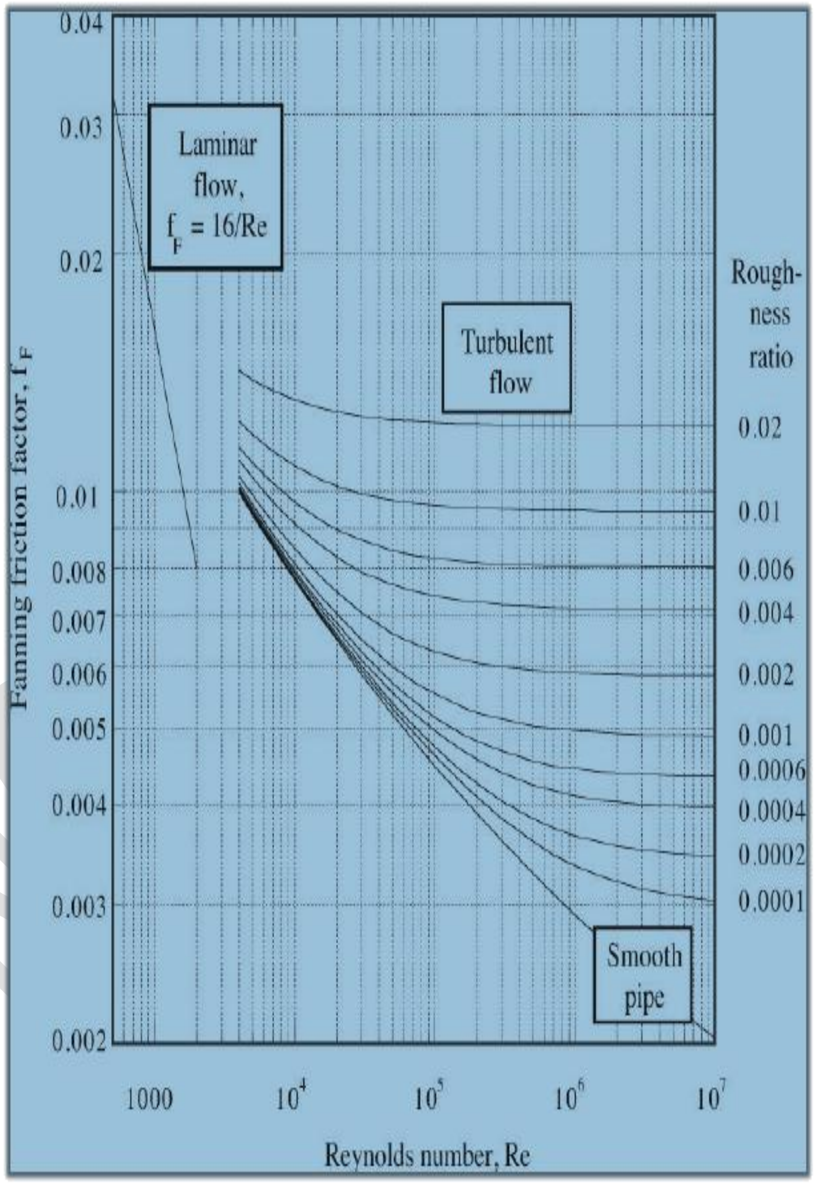

Fig. 11.7 Fanning friction factor for flow in pipes. The turbulent region is based on the Colebrook

Note the following:

1. For *laminar flow* (Re ≤ 2,000 approximately), Eqn. (11.33) is obeyed.

2. In the *transition* region (2,000 < Re ≤ 4,000 approximately), there is no definite correlation, and f_F cannot be given a value. Because of this uncertainty, pipe designs in this region should be avoided.

3. In *turbulent* flow (Re > 4,000), there is a family of curves, with f_F increasing as the relative roughness ε/D increases. Except for smooth pipes (see below), f_F becomes independent of Re a thigh Reynolds numbers.

11.3.1 Pipe roughness.

The question immediately arises as to how a roughness length scale ε can be assigned to the surface of a particular wall material. The situation is idealized in Fig. 11.8, where ε is the diameter of the sand grains.

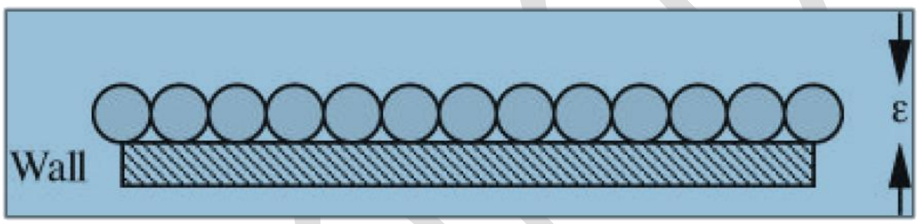

Fig. 11.8 Artificially roughened wall.

Nikuradse then deduced the friction factor for a large number of cases and was able to build up a friction-factor plot for artificially roughened pipes that was very similar to those shown in Fig. 11.7 for "real" surfaces. By comparing the two plots, it is then simple to assign an effective value of ε/D and, hence, ε for a "real" surface. Representative values are given in Table 11.2 for a variety of surfaces.

Table11.2 Effective Surface Roughnesses

Surface	**ε (ft)**	**ε (mm)**
Concrete	0.001-0.01	0.3-3.0
Cast iron	0.00085	0.25
Galvanized iron	0.0005	0.15
Commercial steel	0.00015	0.46
Drawn tubing	0.000005	0.0015